Draft version May 11, 2018
Typeset using LaTeX **manuscript** style in AASTeX62

Predicted intensities of emission lines listed in Table 1 of Landi et al. 2016

Zihao Yang[1]

[1] *School of Earth and Space Sciences, Peking University,*

100871 Beijing, China;

yangzihao96@pku.edu.cn

1. THE DENSITY AND TEMPERATURE MODELS

We mainly calculate the lines considering three different coronal regions: **quiet sun (QS), coronal hole (CH), active region (AR)**.

For solar coronal emission lines in visible and infrared bands, they are formed by both collisional excitation and photoexcitation. Here we use CHIANTI version 8.0.2 to do the calculation, considering the two processes.

For the abundance factor, we choose the photospheric abundance (Asplund et al. 2009) as in Del Zanna et al. (2018).

1.1. *Models used for QS*

1.1.1. *Electron density model*

Adapted from Gibson et al. (1999):

$$n_e = (a * r^{-b} + c * r^{-d} + e * r^{-f}) * 10^8 \ cm^{-3}$$

with $a = 3.6, b = 15.3, c = 0.99, d = 7.34, 3 = 0.365, f = 4.31$

1.1.2. *Electron temperature model*

Assuming the temperature remains $\log T = 6.2$ below $1.5R_{sun}$, after that, adapting the model of Vasquez et al. (2003):

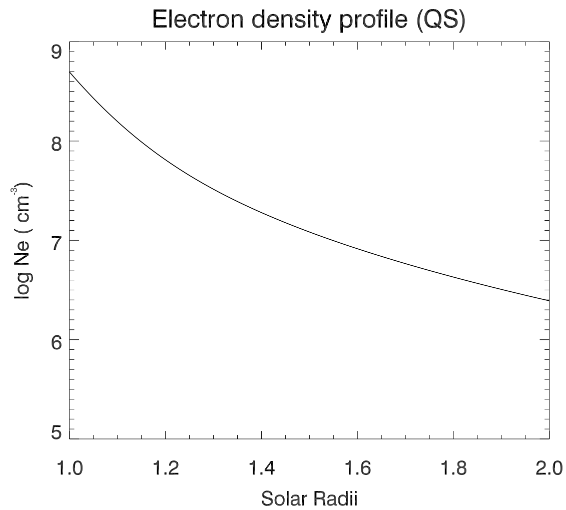

(a) QS

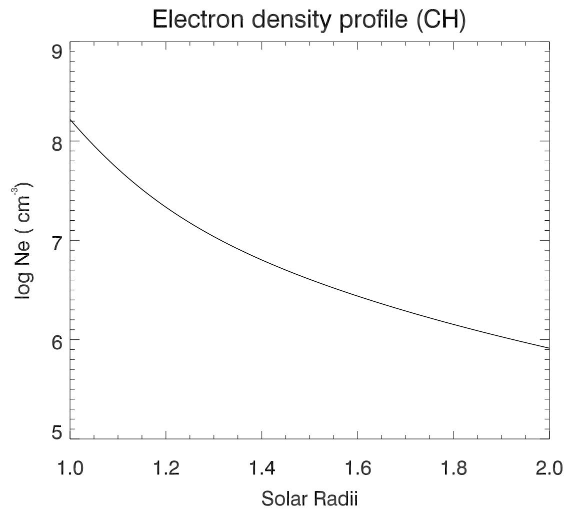

(b) CH

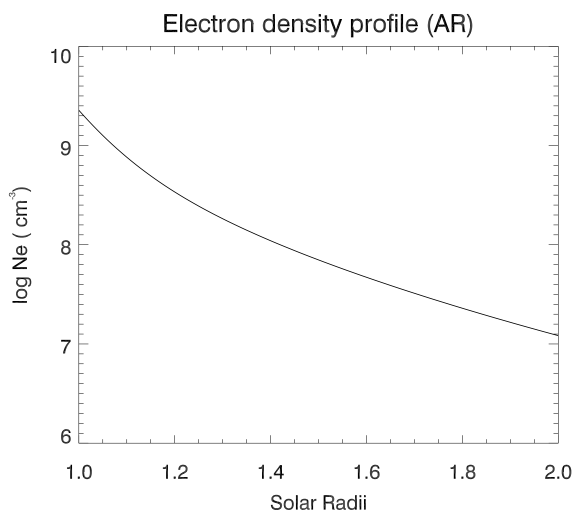

(c) AR

Figure 1. Electron density profiles used in the calculation

$$T = T_0 \frac{\alpha + 1}{\alpha + \beta * r^a + (1 - \beta) * r^{-b}}$$

with $T_0 = 8 \times 10^5 K, \alpha = 0.1, \beta = 0.33, a = 0.55, b = 6.6$

1.2. *Models used for CH*

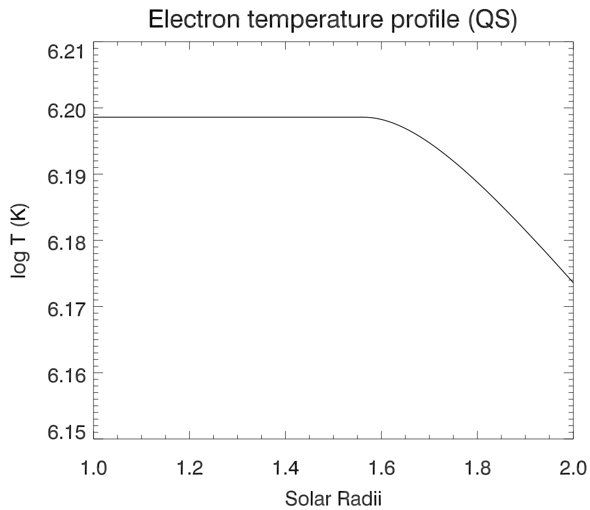

(a) QS

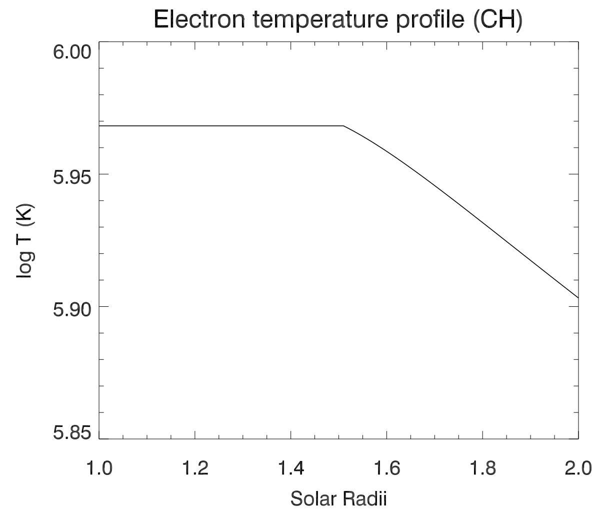

(b) CH

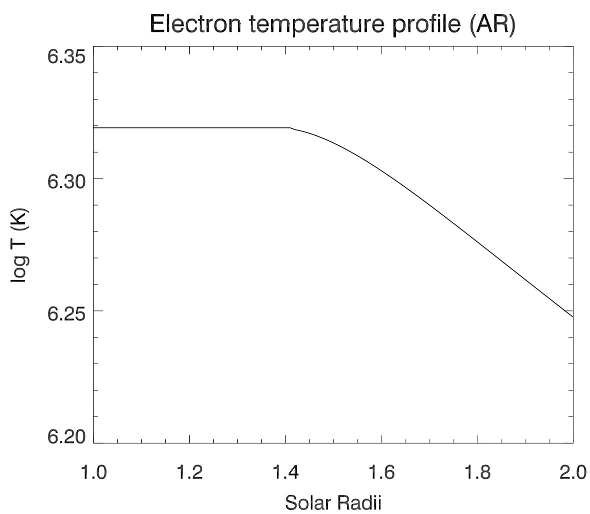

(c) AR

Figure 2. Electron temperature profiles used in the calculation

1.2.1. *Electron density model*

The model is multiplying the QS model with a factor of $\frac{1}{3}$.

1.2.2. *Electron temperature model*

Assuming the temperature remains $\log T = 5.97$ below $1.5R_{sun}$, after that, using the model that multiplying the QS model with a factor of $\frac{1}{1.3}$ so that at any altitude the temperature won't exceed 1MK.

NOTE: *There may be a discontinuity (a bump) in the CH line intensity profile, which is caused by the assumption that before $1.5R_{sun}$ the temperature remains the same.*

1.3. *Models used for AR*

1.3.1. *Electron density model*

$$n_e = 10^8 * (2.99 * r^{-16} + 1.55 * r^{-6}) * 5$$

1.3.2. *Electron temperature model*

Assuming the temperature remains $\log T = 6.32$ below $1.4R_{sun}$, after that, using the model that multiplying the QS model with a factor of 1.7.

NOTE: *the corona above solar active region is usually multithermal, but here we assume it is isothermal, which may lead to results that are deviated from the real situations.*

2. INTENSITIES OF DIFFERENT LINES

2.1. *Fe*

2.1.1. *Fe* VI 5177Å

Fe VI 5177Å, $\log T_{eff} = 4.95 - 5.52$

2.1.2. *Fe* XIV 5303Å

Fe XIV 5303Å, $\log T_{eff} = 6.15 - 6.49$

2.1.3. *Fe* X 6374Å

2.1.4. *Fe* XV 7062Å

Fe XV 7062Å, $\log T_{eff} = 6.20 - 6.63$

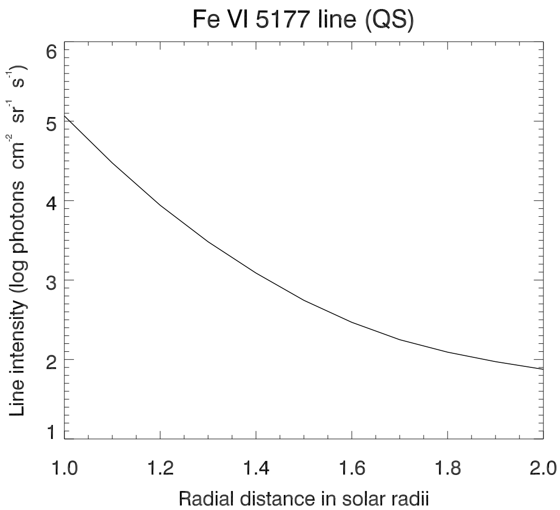

(a) Fe vi 5177 QS

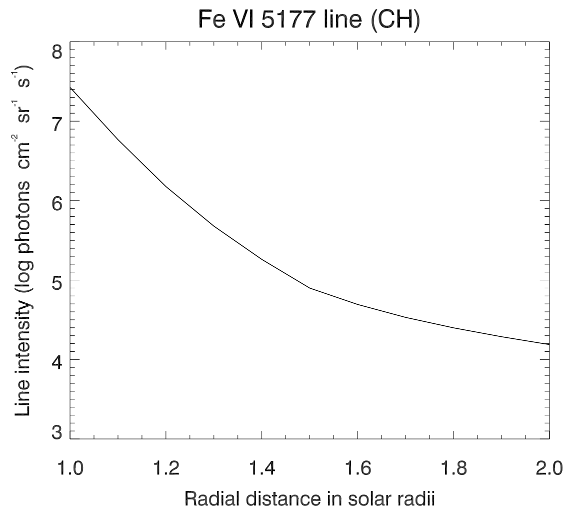

(b) Fe vi 5177 CH

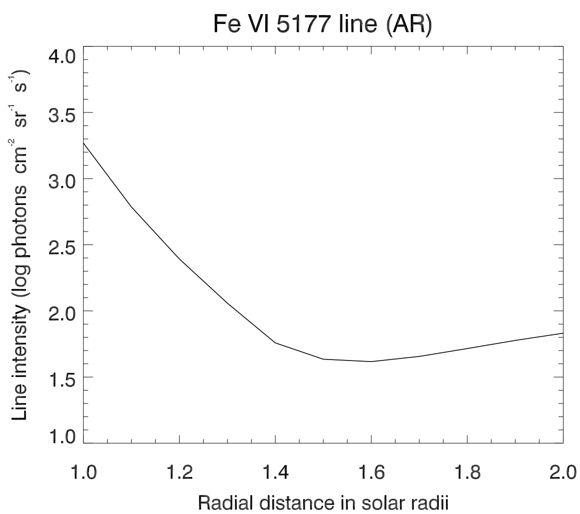

(c) Fe vi 5177 AR

Figure 3. Fe vi 5177

2.1.5. *Fe* xi 7894Å

Fe xi 7894Å, $\log T_{eff} = 5.92 - 6.30$

2.1.6. *Fe* xiii 10747Å

Fe xiii 10747Å, $\log T_{eff} = 6.08 - 6.41$

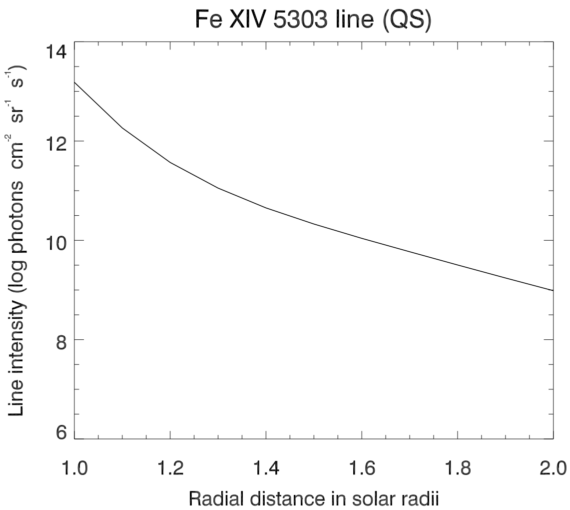

(a) Fe xiv 5303 QS

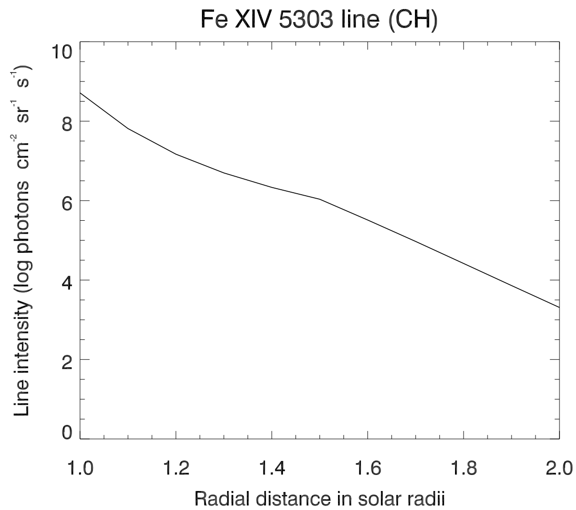

(b) Fe xiv 5303 CH

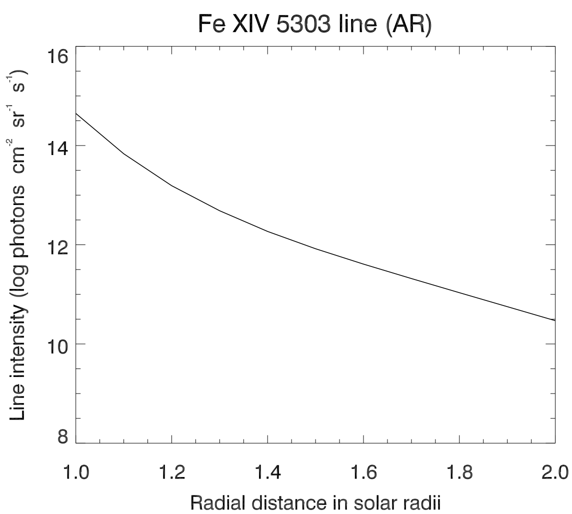

(c) Fe xiv 5303 AR

Figure 4. Fe xiv 5303

2.1.7. *Fe* xiii 10800Å

Fe xiii 10800Å, $\log T_{eff} = 6.08 - 6.41$

2.2. *Ar*

2.2.1. *Ar* x 5535Å

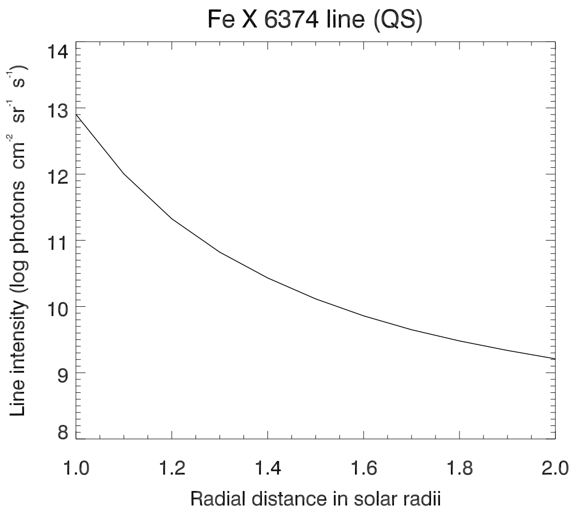

(a) Fe x 6374 QS

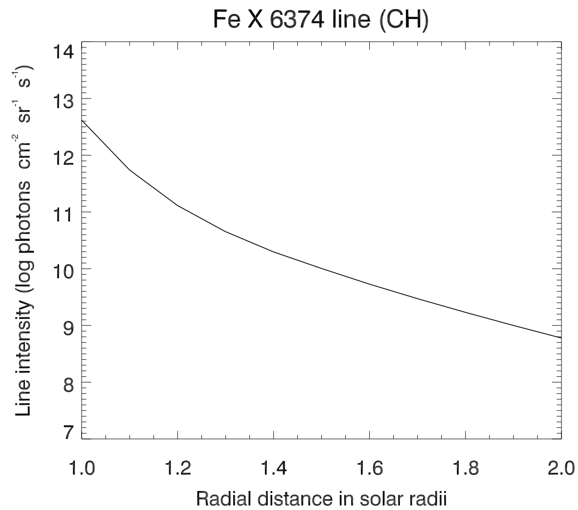

(b) Fe x 6374 CH

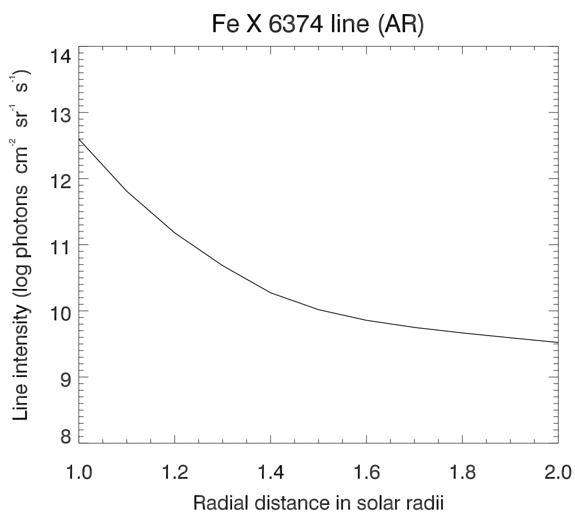

(c) Fe x 6374 AR

Figure 5. Fe x 6374

Ar x 5535Å, $\log T_{eff} = 5.86 - 6.42$

2.2.2. *Ar* xi 6918Å

Ar xi 6918Å, $\log T_{eff} = 6.04 - 6.52$

2.2.3. *Ar* xiii 8339Å

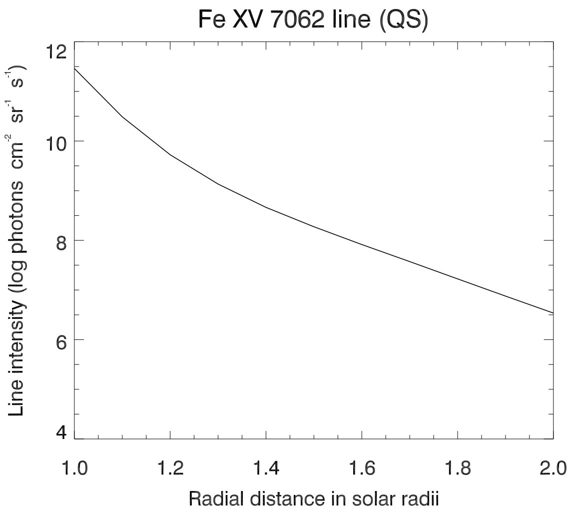

(a) Fe xv 7062 QS

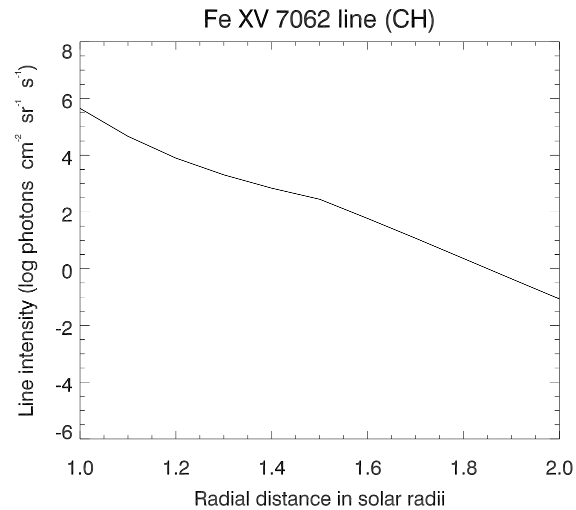

(b) Fe xv 7062 CH

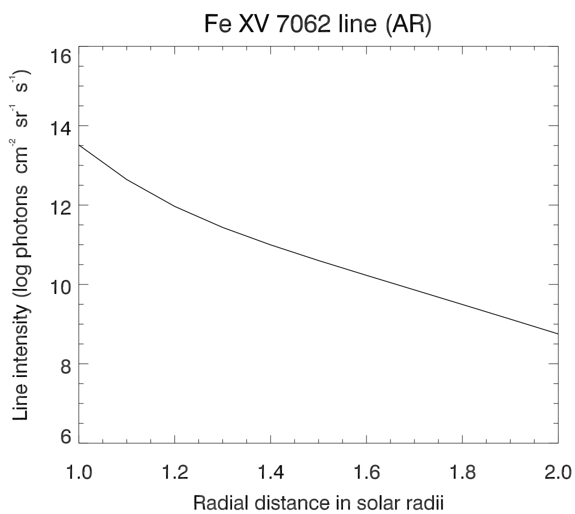

(c) Fe xv 7062 AR

Figure 6. Fe xv 7062

Ar xiii 8339Å, $\log T_{eff} = 6.26 - 6.67$

2.2.4. *Ar* xiii 10143Å

Ar xiii 10143Å, $\log T_{eff} = 6.26 - 6.67$

2.3. *Ca*

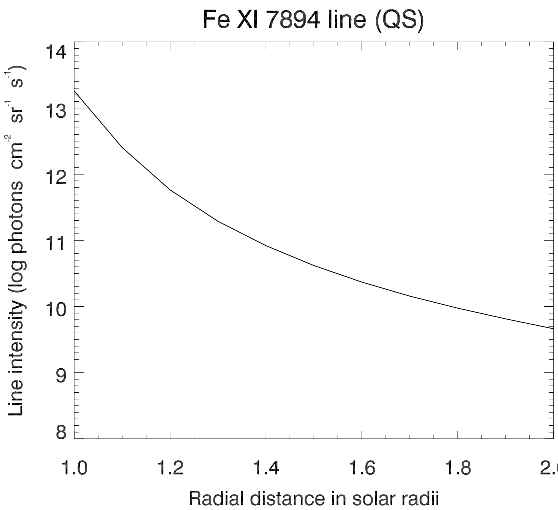

(a) Fe XI 7894 QS

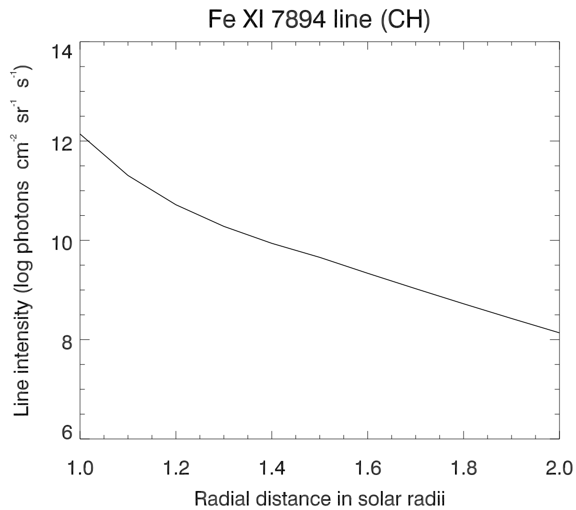

(b) Fe XI 7894 CH

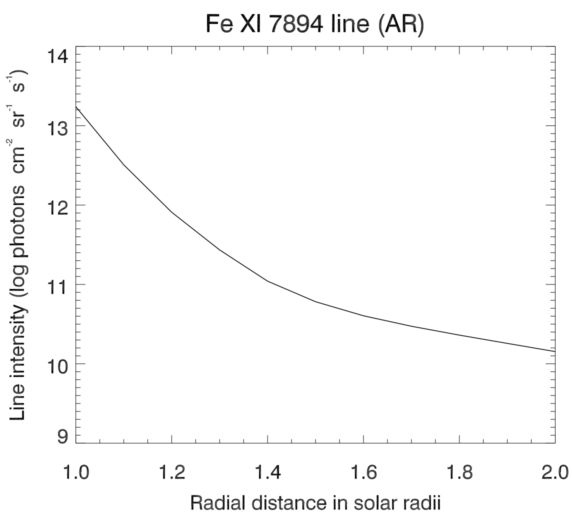

(c) Fe XI 7894 AR

Figure 7. Fe XI 7894

2.3.1. *Ca* XV 5446Å

Ca XV 5446Å, $\log T_{eff} = 6.44 - 6.84$

2.3.2. *Ca* XV 5695Å

Ca XV 5695Å, $\log T_{eff} = 6.44 - 6.84$

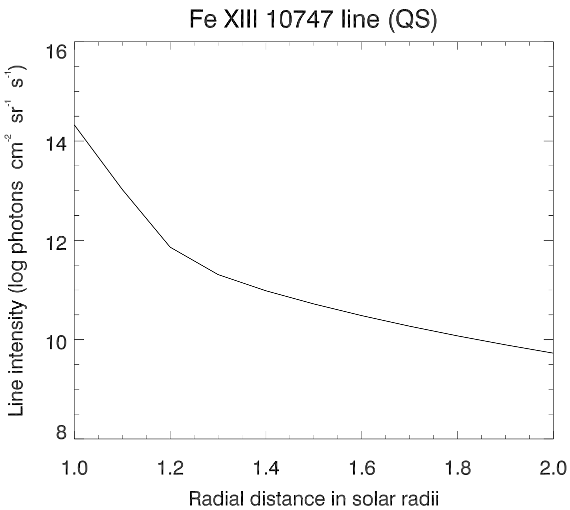

(a) Fe XIII 10747 QS

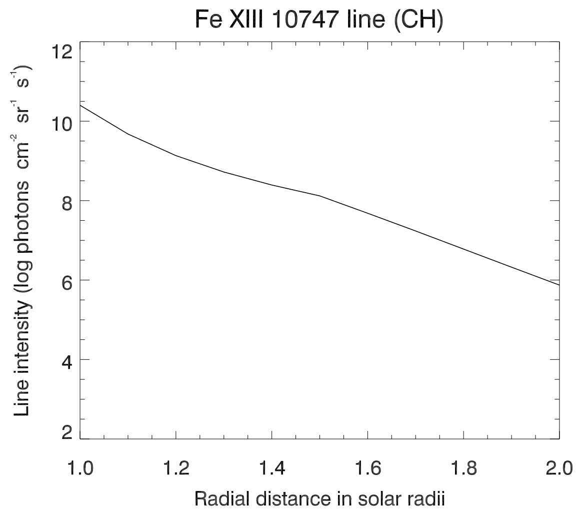

(b) Fe XIII 10747 CH

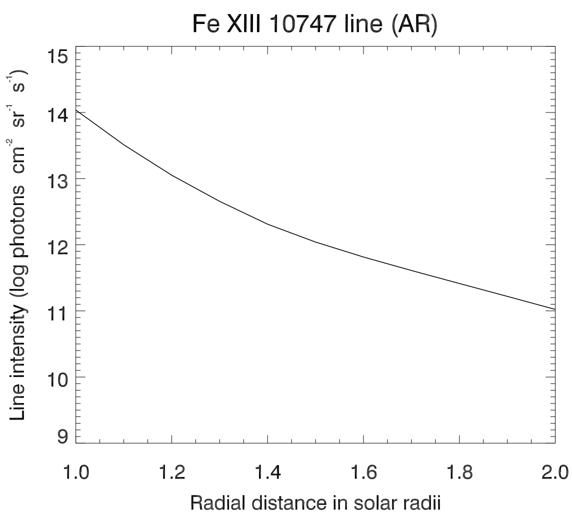

(c) Fe XIII 10747 AR

Figure 8. Fe XIII 10747

2.4. *Others*

2.4.1. *S* XII 7613Å

S XII 7613Å, $\log T_{eff} = 6.16 - 6.55$

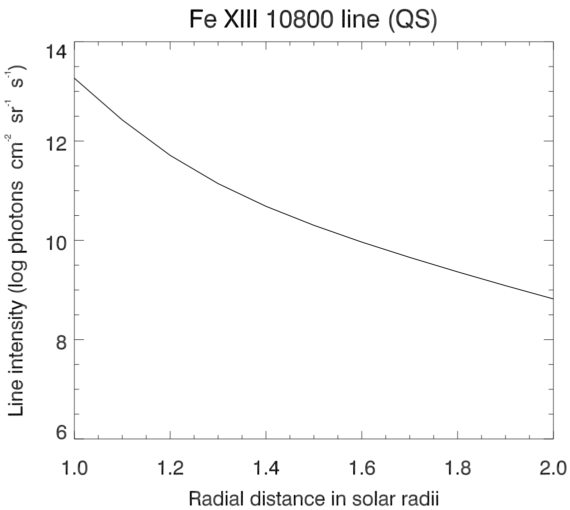

(a) Fe XIII 10800 QS

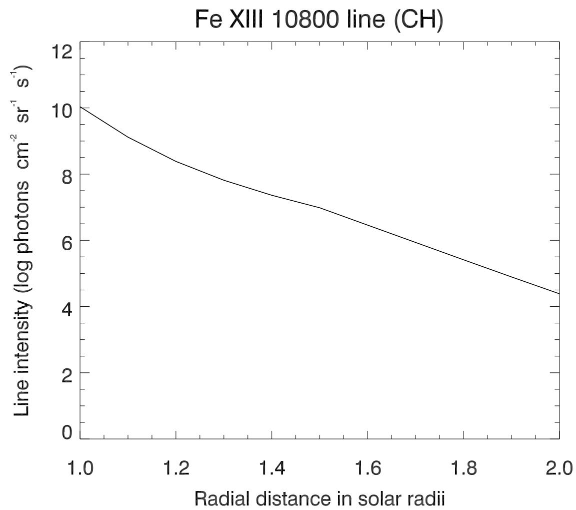

(b) Fe XIII 10800 CH

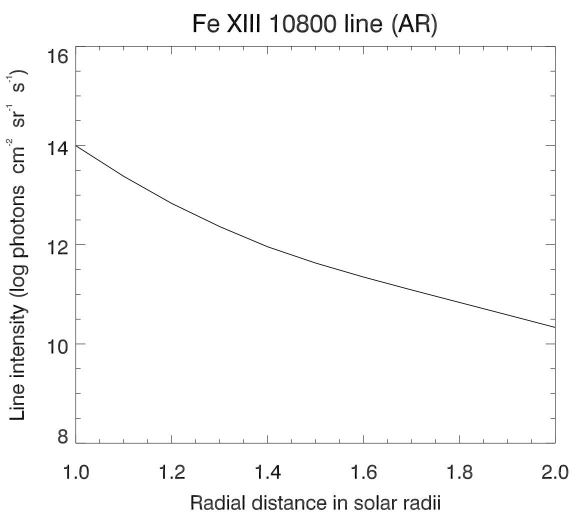

(c) Fe XIII 10800 AR

Figure 9. Fe XIII 10800

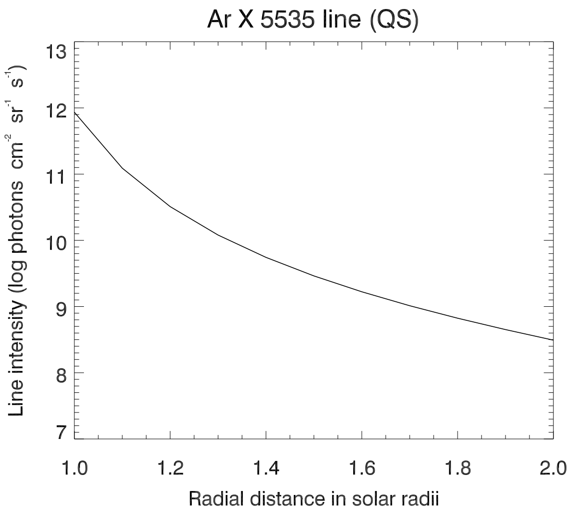

(a) Ar x 5535 QS

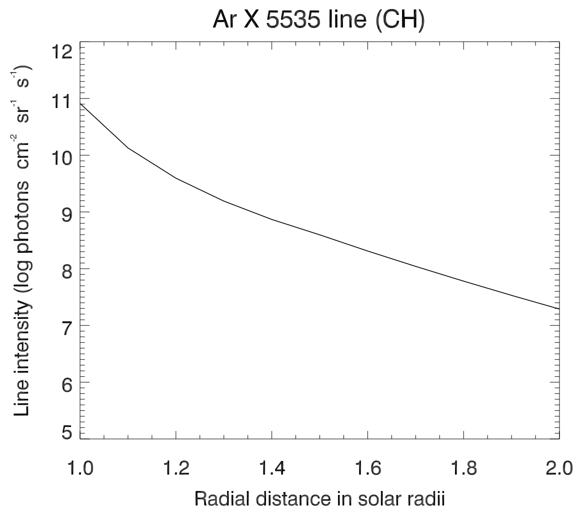

(b) Ar x 5535 CH

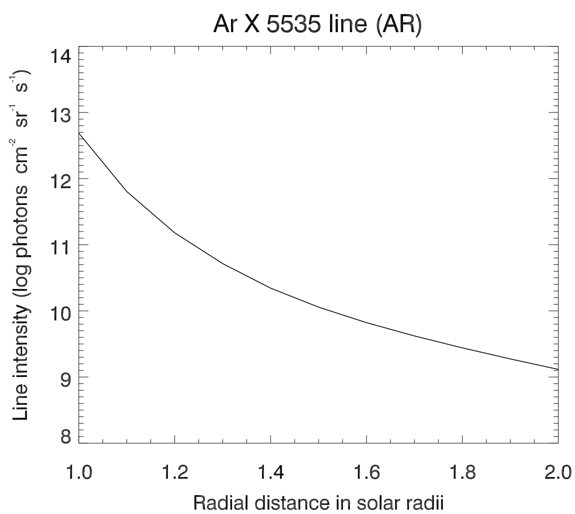

(c) Ar x 5535 AR

Figure 10. Ar x 5535

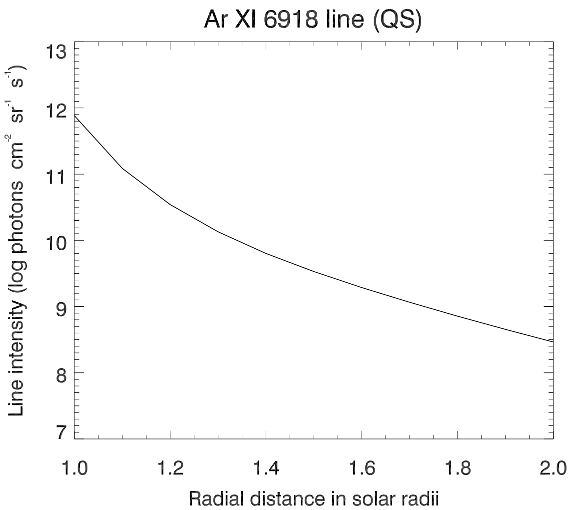

(a) Ar XI 6918 QS

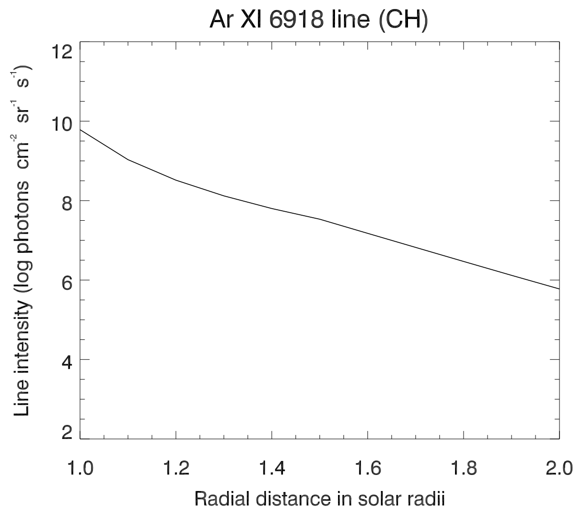

(b) Ar XI 6918 CH

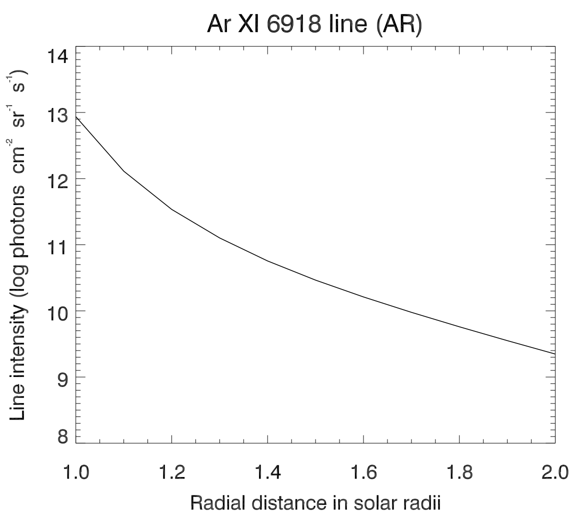

(c) Ar XI 6918 AR

Figure 11. Ar XI 6918

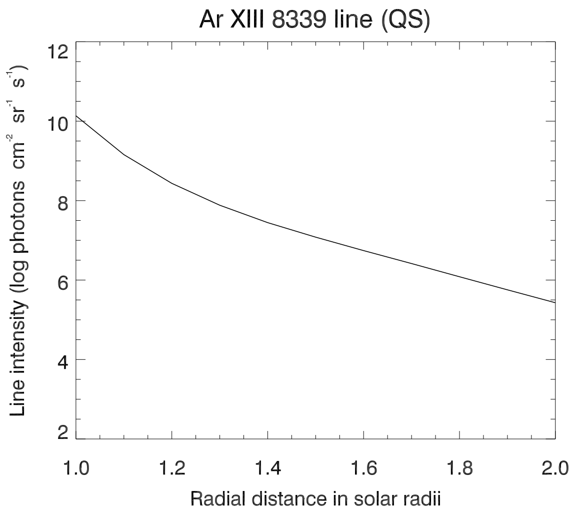

(a) Ar XIII 8339 QS

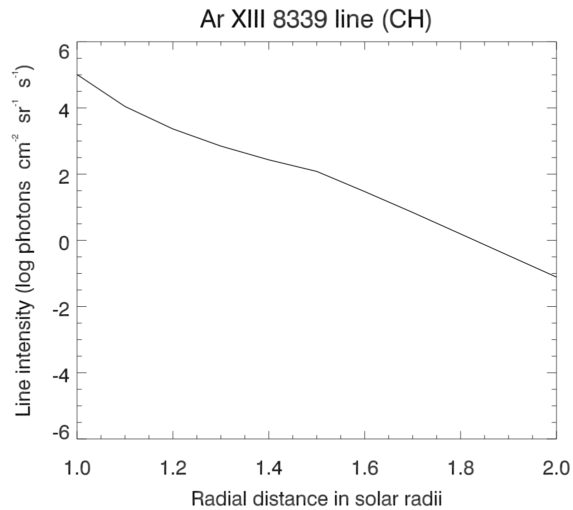

(b) Ar XIII 8339 CH

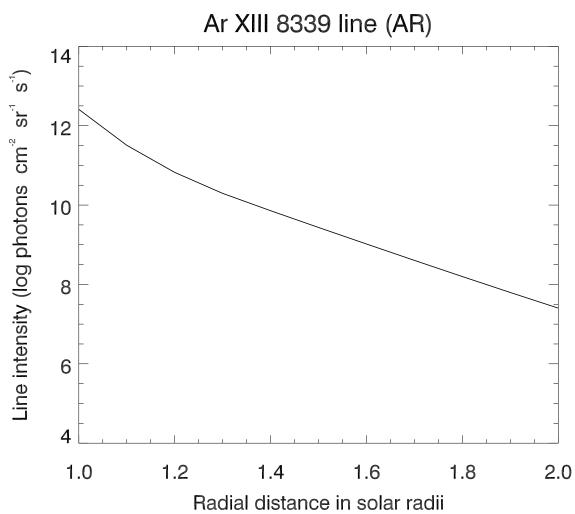

(c) Ar XIII 8339 AR

Figure 12. Ar XIII 8339

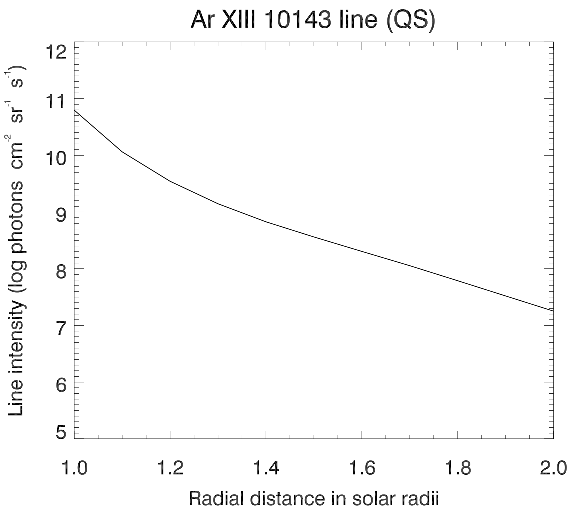

(a) Ar XIII 10143 QS

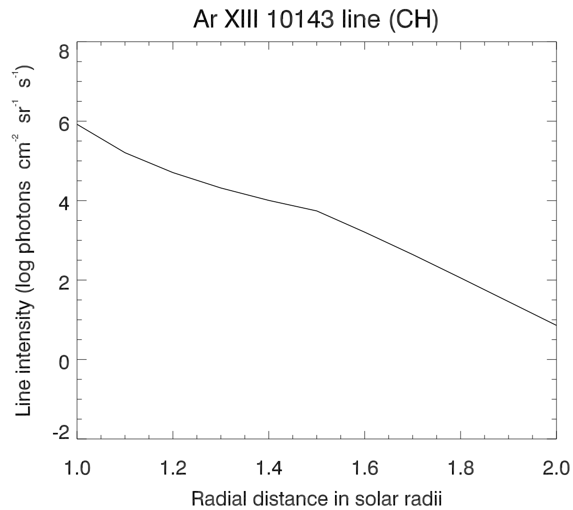

(b) Ar XIII 10143 CH

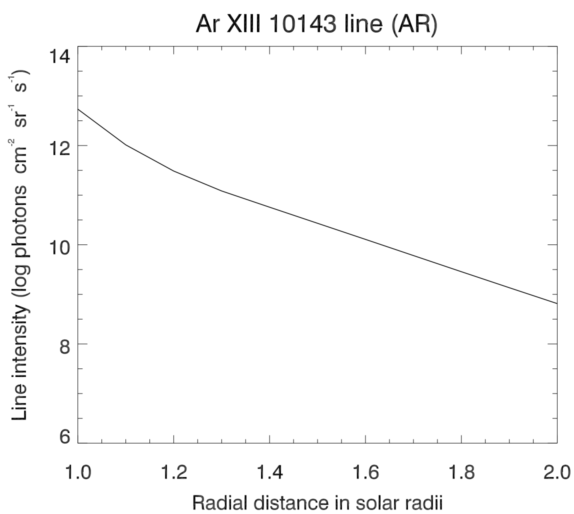

(c) Ar XIII 10143 AR

Figure 13. Ar XIII 10143

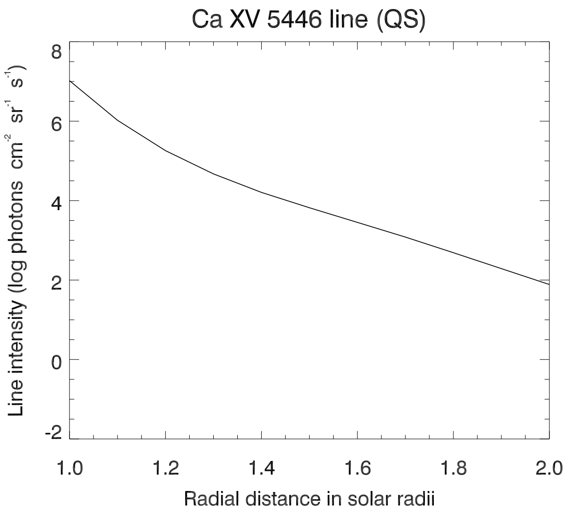

(a) Ca xv 5446 QS

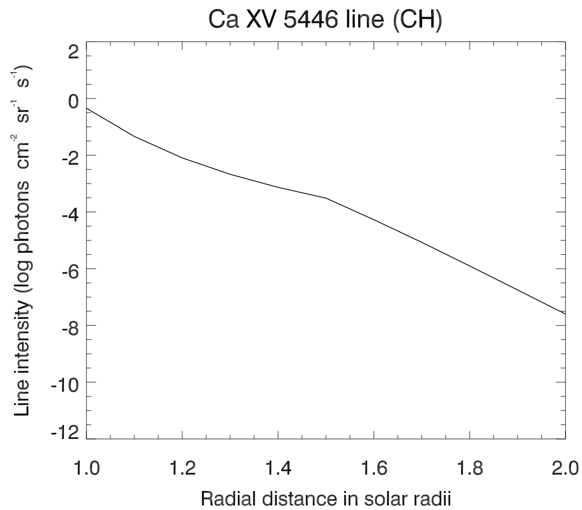

(b) Ca xv 5446 CH

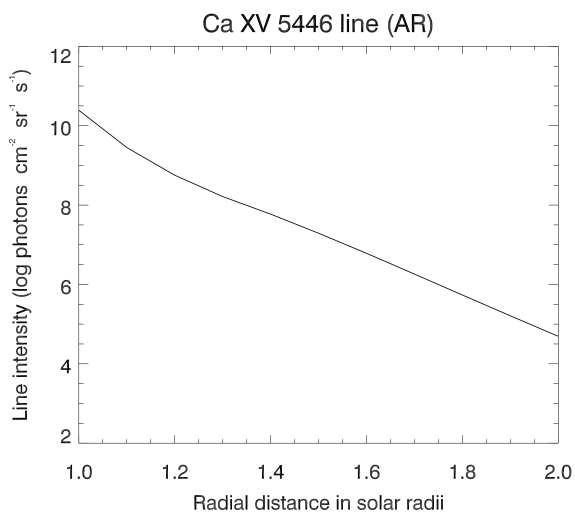

(c) Ca xv 5446 AR

Figure 14. Ca xv 5446

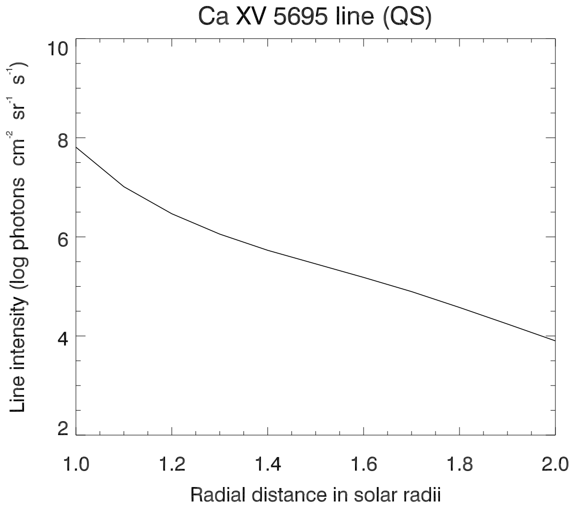

(a) Ca xv 5695 QS

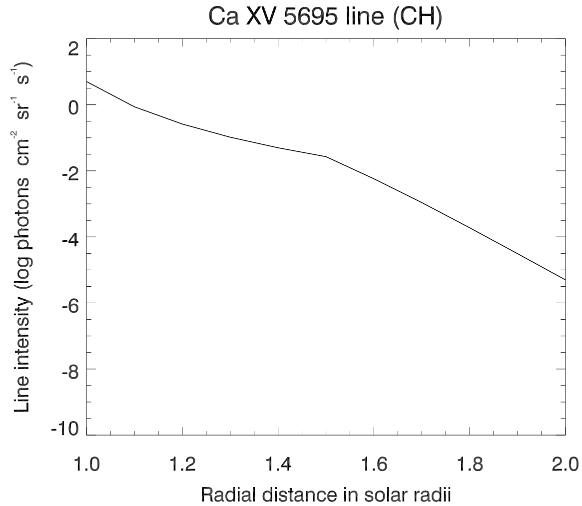

(b) Ca xv 5695 CH

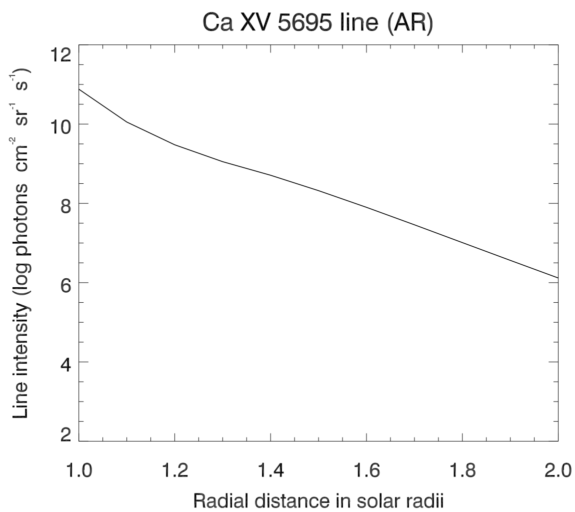

(c) Ca xv 5695 AR

Figure 15. Ca xv 5695

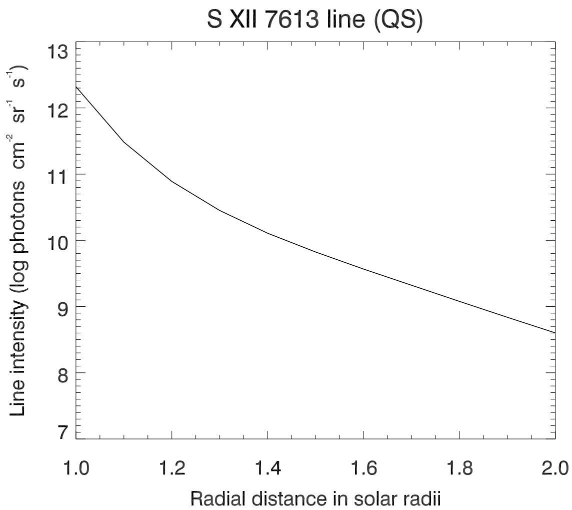

(a) S xii 7613 QS

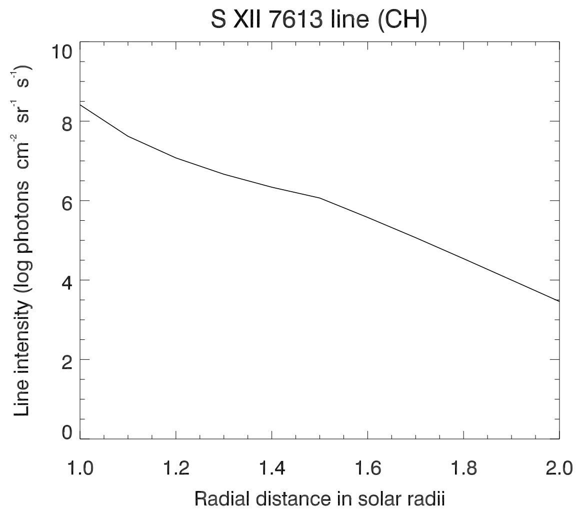

(b) S xii 7613 CH

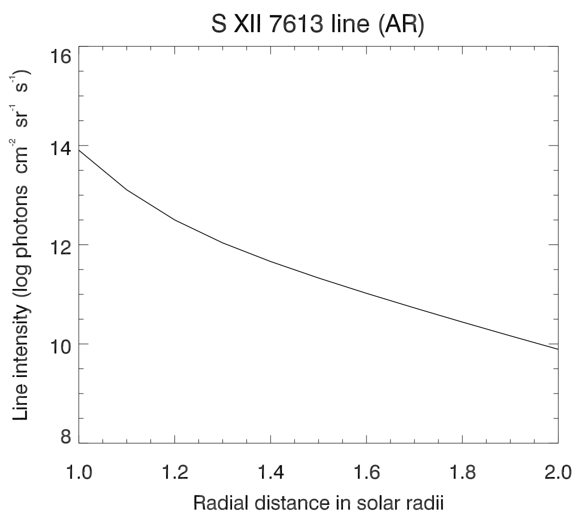

(c) S xii 7613 AR

Figure 16. S xii 7613